

FRACTURE MECHANICS MODELS FOR THE ANALYSIS OF COMPOSITE MATERIALS WITH A NONLINEAR MATRIX

A. Carpinteri, G. Ferro & G. Ventura

Department of Structural Engineering, Politecnico di Torino, 10129, Torino, Italy.

ABSTRACT

A model for reproducing the constitutive flexural response of a fiber-reinforced composite material with a non-linear matrix is proposed. The nonlinearity of the matrix is modelled by considering a distribution of closing forces onto the crack faces which increases the fracture toughness of the cross-section with a shielding action. The constitutive flexural response depends on three dimensionless parameters: \tilde{w}_c^E , which controls the extension of the process zone, $N_P^{(1)}$ and $N_P^{(2)}$, called *brittleness numbers*, which are related to the reinforcement phases. The role of the specimen size scale is fundamental for the global structural behaviour, which can range from ductile to brittle simply with the variation of the two brittleness numbers. They are functions of matrix toughness, reinforcement yielding or slippage limit, reinforcement volume fraction and global structural size. The application of the model to steel bar reinforced high-performance concrete with fibers is in good agreement with the experimental results.

KEYWORDS

Fracture mechanisms, Fiber-reinforced composite material, High-performance concrete, Bridged crack, Size effects.

INTRODUCTION

The development of high-performance composite materials has been playing a key role in the recent engineering applications. In civil engineering, for example, the introduction of high-strength concretes, characterized by a very brittle behaviour, has required the addition of a secondary phase of reinforcement (fibers) to increase the fracture toughness of the material, so that the cementitious matrix assumes a nonlinear constitutive behaviour. The development of high-performance concretes is emblematic for the modern approach to new composite materials. Despite a large proliferation of experimental tests and papers on the structural behaviour of reinforced elements, there are not theoretical models which describe in exhaustive manner these materials. The purpose of this paper is to offer a contribution to the theoretical modelization of the bent elements.

The application of Fracture Mechanics concepts to plain and reinforced concrete structures represents the only way to interpret the collapse behaviour, which shows different rupture modes by varying the size. Two different models have been proposed in the last few years to describe partial damage near a single crack: the *cohesive crack model* and the *bridged crack model*. In the former, the stress-intensity factor K_I at the crack tip is set equal to zero due to the contribution of the applied load and of the softening tractions acting ahead of the notch. The first application to brittle materials is due to Barenblatt [1], while important contributions to relate the cohesive model to the Griffith crack are due to Willis [2] and Rice [3]. In the *bridged crack model* the near tip process is modeled via the stress-intensity factor and a crack propagation condition is reached when the stress-intensity factor equals the toughness of the brittle matrix. Several bridged crack models have been proposed to simulate the structural response of fiber-reinforced materials. These models have been used to describe cracking in brittle-matrix composites [4] and in alloy plates shielded by bonded patches [5], as well as damage zones in concrete [6].

The theoretical model to which we refer determines the problem unknowns by considering the cracked cross-section and by using the local compliance and the stress-intensity factor concepts. It represents an extension of the model proposed by Carpinteri [7] for one single reinforcement, by Bosco and Carpinteri [8] for a discontinuous fiber distribution and by Carpinteri and Massabò [9] for a continuous distribution. The longitudinal

(primary) reinforcements are simulated by the actions of m concentrated forces directly applied onto the crack faces. The nonlinearities of the matrix are instead modelled by the action of a continuous closing traction distribution (secondary reinforcement) onto the cracked zone. Alternatively, the model can simulate a composite material with a brittle matrix and two level of reinforcements, so that it can also be applied to a wider class of composite materials [10]. For the crack propagation condition, both the bridging option as well as the cohesive one are introduced.

The structural response expressed by the functional relationship moment versus local rotation, i.e. M vs ϕ , comes out from Dimensional Analysis [10] of the bridging option to depend on three dimensional parameters:

$$\tilde{w}_c^E = \frac{Ew_c}{K_{IC}h^{0.5}}; \quad N_P^{(1)} = \frac{\rho\sigma_y h^{0.5}}{K_{IC}}; \quad N_P^{(2)} = \frac{\gamma\sigma_u h^{0.5}}{K_{IC}}, \quad (1)$$

where the symbols are described in the next section. In the cohesive option the third parameter assumes a different expression, as reported later. The parameter \tilde{w}_c^E , is a function of the kind of fibers used, and specifically of their length. The other two parameters, called *brittleness numbers*, are related to the two levels of reinforcements. The structural response depends, once all the other mechanical parameters have been set, on the structural element dimension. Theoretical results confirm a transition from brittle to ductile collapse by increasing the brittleness numbers N_P . It is to be observed that the dependence of the brittleness numbers on the structural dimension is represented by a power law with an exponent equal to 0.5, typical for the Linear Elastic Fracture Mechanics stress singularity. A comparison of the theoretical curve vs the experimental one in the case of an high-strength concrete with the two reinforcement phases is discussed at the end of the paper for emphasizing the consistency of the model.

THEORETICAL MODELS

The theoretical model explains and reproduces the constitutive flexural response of a fiber-reinforced concrete element with longitudinal steel bars. Two different options for the model can be used, the *bridging* and the *cohesive*. The scheme of a cracked element is shown in fig. 1.a, where h and b are the height and the width of the cross-section. The normalized crack depth $\xi = a/h$ and the normalized coordinate $\zeta = x/h$ are defined, x being the generic coordinate related to the bottom of the cross-section. In the *bridging option*, the distribution of the discrete actions P_i and of the continuous closing tractions $\sigma(w)$, directly applied onto the crack faces, respectively represent the physical bridging mechanisms of the longitudinal bars (primary reinforcement) and of the fibers (secondary reinforcement), acting at two different scales. Let c_i be the coordinate of the i th reinforcement from the bottom of the beam, and $\zeta_i = c_i/h$ its normalized value. Function $\sigma(w)$ is a constitutive law and defines the relation between the bridging tractions, representative of the action exerted by the fibers onto the crack, and $w(x)$, the crack opening displacement at the generic coordinate x . The cohesive law σ versus w can be extrapolated from experimental pull-out tests on a single fiber. For the sake of simplicity, in the simulation presented herein a perfectly-plastic law with vertical drop for the fibers has been used, Fig.1.c, even if a general law could also be considered. The bridging forces of the secondary reinforcement act on the portion of the crack whose opening displacement is less than the critical value w_c , beyond which the closing tractions vanish (fig. 1.c). In the *cohesive option*, instead, the brittle matrix and the fibers are represented as a single-phase material with homogenized properties. In this case, the closing tractions $\sigma(w)$ describe the combined restraining action of the matrix and of the fibers on the crack propagation and are given by the cohesive law of the composite material.

The assumed rigid-plastic bridging relation for the crack opening displacement w_i at the level of the i th reinforcement is suitable to describe both the yielding mechanism for the reinforcement and the bar-matrix relative slippage (fig. 1.b). The maximum bridging traction is defined for the primary reinforcements by the ultimate force $P_{Pi} = A_i\sigma_y$ and for the fibers by the ultimate stress $\sigma_0 = \gamma\sigma_u$, A_i being the single reinforcement cross-section area, γ the fibers volume ratio, σ_y or σ_u the minimum between the reinforcement yield strength and the sliding limit for the two reinforcement phases. The stress-intensity factors K_{IM} due to the bending moment M , $K_{I\sigma}$ due to the fibers and K_{Ii} due to the i th-longitudinal reinforcement, can be expressed in accordance with the two-dimensional single-edge notched-strip solution [11]:

$$K_{IM} = \frac{M}{bh^{1.5}}Y_M(\xi) \quad (2)$$

$$K_{I\sigma} = \int_0^\xi \frac{K_{Ij}}{P_j} \sigma(w(\zeta_j))bh \, d\zeta_j = \frac{1}{h^{0.5}b} \int_0^\xi \sigma(w(\zeta_j))Y_P(\xi, \zeta)bh \, d\zeta_j \quad (3)$$

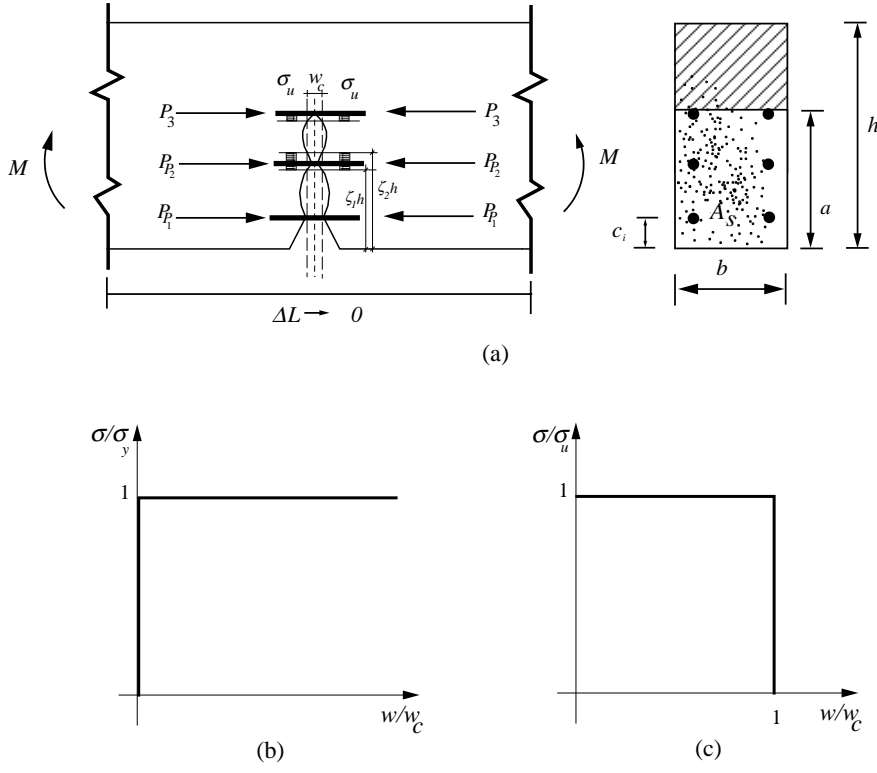


Figure 1: (a) Scheme of a cracked reinforced concrete element containing fibers; (b) rigid-perfectly plastic law for primary reinforcement; (c) plastic law with vertical drop for secondary reinforcement.

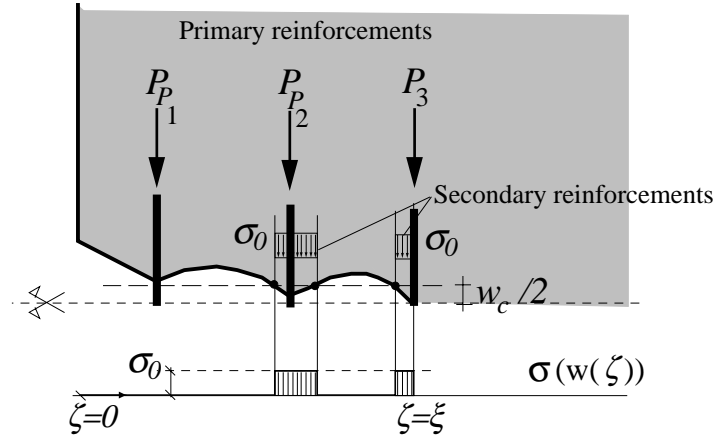


Figure 2: Bridging actions of primary and secondary reinforcements onto the crack faces.

$$K_{Ii} = \frac{P_i}{bh^{0.5}} Y_P(\xi, \zeta_i) \quad (i = 1, 2, \dots, m), \quad (4)$$

where $Y_M(\xi)$ and $Y_P(\xi, \zeta_i)$ are functions of the relative crack depth ξ . $K_{I\sigma}$ is obtained by integrating, along the bridged crack zone, the product of the stress-intensity factor due to two opposite unit forces, applied at the generic coordinate ζ_j , times the bridging actions $\sigma(w)$. The integration is extended to the whole crack while function $\sigma(w)$ assumes nonzero values only where $w < w_c$.

The crack propagates when K_I is equal to the matrix fracture toughness, K_{IC} , for the *bridging* option and when K_I vanishes for the *cohesive* one:

$$K_I = K_{IM} - \sum_{j=1}^m K_{Ij} - K_{I\sigma} = \begin{cases} K_{IC}, & \text{bridging option (singular stress field at the crack tip)} \\ 0, & \text{cohesive option (finite stress field at the crack tip)} \end{cases} \quad (5)$$

The dimensionless crack propagation moment can be obtained from eqs (2-5):

$$\frac{M_F}{K_{IC} h^{1.5} b} = \frac{1}{Y_M(\xi)} \left\{ \frac{N_P^{(1)} m}{\rho} \sum_{i=1}^m \rho_i \frac{P_i}{P_{Pi}} Y_P(\xi, \zeta) + B \int_0^\xi \frac{\sigma(w(\zeta))}{\gamma \sigma_u} Y_P(\xi, \zeta) b h d\zeta + K \right\}, \quad (6)$$

where for $K = 1$ (bridging option) $B = N_P^{(2)} = \frac{\gamma\sigma_u h^{0.5}}{K_{IC}}$, while for $K = 0$ (cohesive option) $B = \frac{1}{s} = \frac{\sigma_u h^{0.5}}{K_{IC}}$, where s is the brittleness number originally defined by Carpinteri [12]. The parameters in the two cases assume different physical meaning. In the bridging option, K_{IC} represents the matrix fracture toughness while in the cohesive option it represents the homogenized toughness of the composite; σ_u represents the ultimate strength of the secondary reinforcement in the former case or the homogenized ultimate strength of the composite in the latter. For a generical relation $\sigma(w)$, the fibers closing tractions onto the crack are indeterminate and depend on the crack opening displacement function $w(x)$. The crack profile (fig.2) can be defined as a function of the mechanical and geometrical properties of the cross-section and of the applied loads, through Castigliano's Theorem:

$$w(\zeta_k) = \lim_{F \rightarrow 0} \frac{\partial}{\partial F(\zeta_k)} \left\{ \int_0^\xi \frac{K_I^2}{E} b h \, dy \right\},$$

where $w(\zeta_k)$ is the crack opening displacement at the generic coordinate $\zeta = \zeta_k$, F are two fictitious forces applied in ζ_k and K_I is the global stress-intensity factor:

$$K_I = K_{IM} - \sum_{j=1}^m K_{Ij} - K_{I\sigma} + K_{IF}, \quad (7)$$

in which K_{IF} is the stress-intensity factor due to the forces F . The normalized crack opening displacement assumes the following form, by substituting the expressions of the stress-intensity factors:

$$\tilde{w}(\zeta_k) = \frac{w(\zeta_k)}{h} = \frac{2K_{IC}}{Eh^{0.5}} \left\{ \frac{M_F}{K_{IC}h^{1.5}b} \int_{\zeta_k}^\xi Y_M(y) Y_P(y, \zeta_k) dy - \frac{N_P^{(1)}}{\rho} \sum_{i=1}^m \left[\frac{P_i}{P_{Pi}} \rho_i \int_{\max[\zeta_i, \zeta_k]}^\xi Y_P(\zeta_i, y) Y_P(y, \zeta_k) dy \right] - B \int_{\zeta_k}^\xi \left(\int_0^y \frac{\sigma(w(\zeta))}{\sigma_u} Y_P(y, \zeta) d\zeta \right) Y_P(y, \zeta_k) dy \right\}, \quad (8)$$

in which the last term represents the displacement at the abscissa ζ_k due to the distribution of tractions $\sigma(w)$ between 0 e ξ . The localized rotation ϕ of the cracked cross-section can be evaluated in the same way by using Castigliano's Theorem and the explicit expression can be found in [10]. Equations (6) and (8) set up a statically indeterminate nonlinear problem. The reactions P_i and $\sigma(w)$ are evaluated by using a numerical procedure based on the assessment of kinematical compatibility and statical equilibrium equations. The complete description of the computational algorithm is reported in [10].

NUMERICAL SIMULATIONS

The numerical procedure under the bridging option has been used to evaluate the flexural behaviour of the cross-section reinforced with two different levels of fibers. The three dimensionless numbers, $N_P^{(1)}$, $N_P^{(2)}$ and \tilde{w}_c^E , affect the shape of the curves. Some theoretical diagrams are presented by varying one dimensionless number, the other two being fixed. This is to appreciate the influence of a single group onto the flexural response. A cracked reinforced concrete element containing fibers is considered in the following examples, in which, for the sake of simplicity in the interpretation of the curves, only one primary reinforcement is placed at the normalized coordinate $\zeta_1 = c/h = 0.1$.

As a first case, the evolutive process of crack propagation expressed in terms of the dimensionless crack propagation moment, $M_F/(K_{IC}h^{1.5}b)$, vs the normalized crack depth, $\xi = a/h$, with a fixed value of the primary brittleness number $N_P^{(1)}=1.0$ and a fixed dimensionless critical crack opening displacement $\tilde{w}_c^E=300$, is reported in fig. 3.a, for different values of the secondary brittleness number $N_P^{(2)}$ varying between 0 (no secondary phase reinforcement) and 1.9. For $0 < \xi < \zeta_1$, the crack crosses only the matrix of the cross-section. The strain-softening response is controlled by the matrix toughness and by the secondary reinforcements. For crack depths tending to zero, an infinite resistance is provided, as expected from LEFM. In correspondence of $\xi = \zeta_1 = 0.1$, when the crack reaches the primary reinforcement, a loading drop is evidenced. If all the mechanical as well as the dimensional parameters of the cross-section are fixed, the transition from $N_P^{(2)}=0.0$ to $N_P^{(2)}=1.9$ can be due only to an increment of the fiber content percentage. In such a case, the increment of the fiber percentage increases the toughness of the cross-section, and, secondarily, also the resistance, the curves being translated toward larger values of the crack propagation moment. The circles in the diagram indicate the minimum for each curve, which represents a transition in the evolutive process of crack propagation. For crack depths lower than that corresponding to the minimum, the response is unstable and an uncontrollable crack propagation can be avoided only by progressively decreasing the applied load. On the other hand, for crack depths larger than

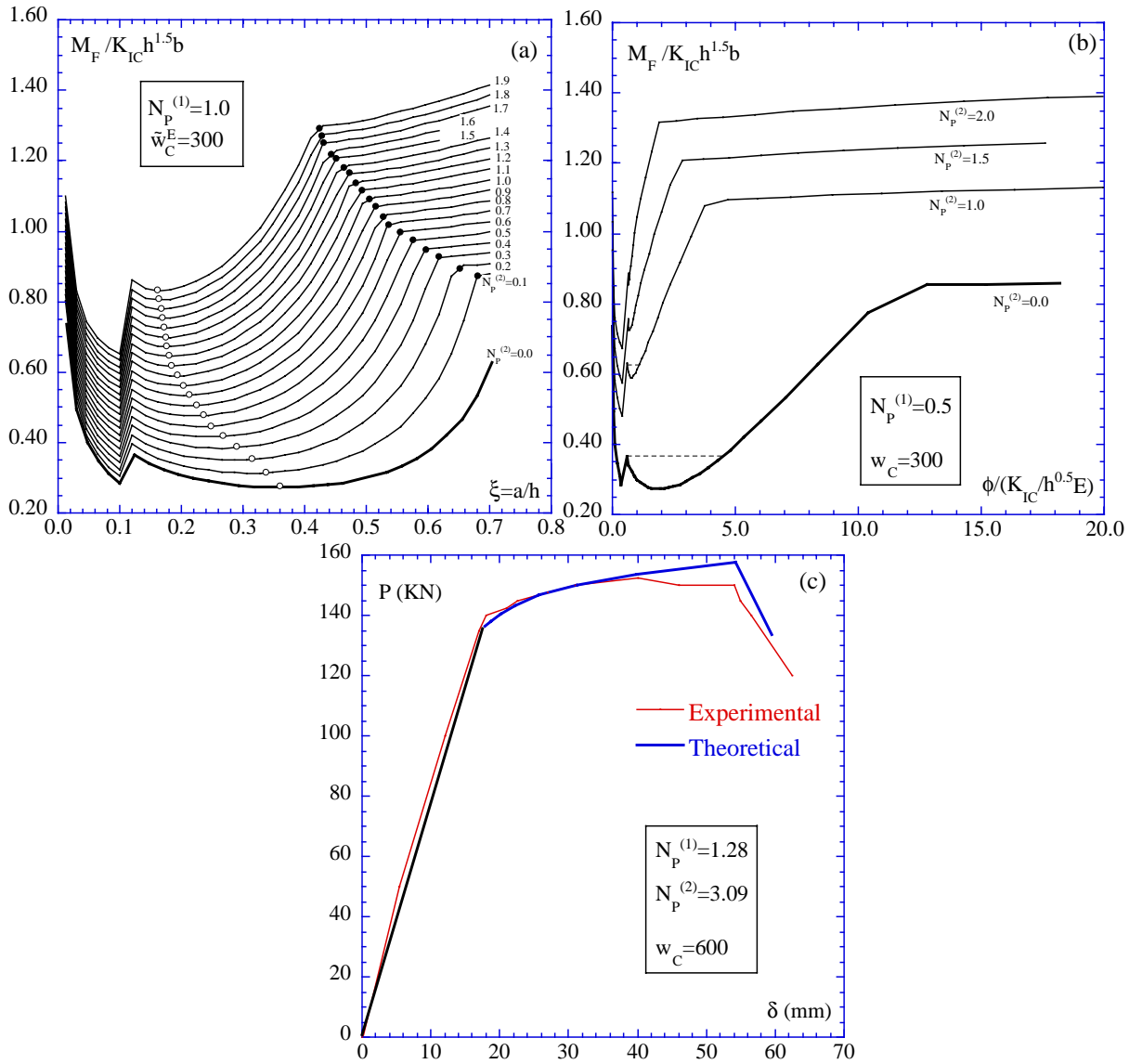


Figure 3: (a) Dimensionless crack propagation moment vs normalized crack depth for fiber-reinforced concrete cross-section with $N_p^{(1)}=1.0$, $\tilde{w}_c^E=300$ and $N_p^{(2)}$ between 0.0 and 1.9. (b) Dimensionless crack propagation moment vs localized rotation diagram for a concrete cross-section as $N_p^{(2)}$ varies, with $N_p^{(1)}=0.5$ and $\tilde{w}_c^E=300$. (c) Comparison between the experimental load-deflection curve for a fiber-reinforced high-strength concrete [14] and the theoretical results (bridging option).

the limit value, the process is stable, and a slow crack growth is possible also by increasing the applied load. The limit crack depth increases when the brittleness number $N_p^{(2)}$ decreases. This result is consistent with the curves obtained by Carpinteri and Massabò [13] for the cross-section with only secondary reinforcement. The dots in the figure indicate the primary reinforcement yielding points. It can be observed how the yielding point translates by varying the secondary brittleness number $N_p^{(2)}$.

From an engineering point of view, it appears very interesting to consider the crack propagation moment vs localized rotation diagram. Fig. 3.b shows the curves for $N_p^{(1)}=0.5$ and $\tilde{w}_c^E=300$ and four different values of $N_p^{(2)}$. The first one ($N_p^{(2)}=0.0$) is representative of a fiber-reinforced concrete cross-section with no secondary reinforcement. The crack propagation moment shows a vertical asymptote for $\phi \rightarrow 0$ ($\xi \rightarrow 0$). A vertical drop is achieved when the crack crosses the primary reinforcement. For $N_p^{(2)}=0.0$ and 1.5, a snap-through instability is present after the drop (dotted line), which is less and less evident for increasing values of $N_p^{(2)}$.

The proposed theoretical model has been assessed by simulating an experimental test carried out by Ashour and Wafa [14] on high-strength concrete beams with the presence of two steel bar reinforcements. The beams, loaded in a four-point bending scheme, have a depth \times thickness \times span of 170 \times 300 \times 3680 mm. In the testing programme, 20 mm Grade 60 deformed steel bars having yield strength of 437 MPa were used as flexural reinforcement. The concrete mix proportion was 1:0.25:2.5 (cement:sand:coarse aggregate) to produce concrete

with a compressive strength of about 88 MPa. The Young's modulus has been evaluated to be 38,000 N/mm², while no information for unreinforced matrix fracture energy is available. Hooked-ends mild carbon steel fibers were used with average length of 60 mm, nominal diameter of 0.8 mm, aspect ratio of 75, and yield strength of 1100 MPa, with a fiber content of 1.5 %. By supposing a matrix fracture toughness equal to 0.14 Nmm^{-3/2} for the present case, we obtain $N_P^{(1)}=1.276$, $N_P^{(2)}=3.0928$ and $\tilde{w}_c^E=600$, having supposed $w_c=1/3$ of the length of the fiber. In order to evaluate the load-deflection theoretical curves, the constitutive moment vs localized rotation [10] has been used as a nonlinear hinge placed in the middle of the free span of the four point linear elastic beam [15]. Fig. 3.c shows the relationship between the applied load P and the middle-span deflection δ . The thin curve represents the experimental result, while the thick curve represents the theoretical one. After the linear elastic portion, an hardening behaviour appears due to the yielding of the primary reinforcement and to the bridging action of the fibers. Then, a softening behaviour is evidenced, due to the brittle failure (vertical drop) of the secondary fibers. It can be noticed a very small difference between the two curves, and only in the final portion, when the primary reinforcement yields, an error of 5 % has been achieved.

CONCLUSIONS

The proposed model represents an extension of the bridged crack model to the concurrent presence in a cementitious matrix of longitudinal bars and uniformly distributed fibers. A cohesive crack version can be obtained. It has been shown that the flexural behaviour of geometrically similar structures is governed by three dimensionless parameters. The influence of each parameter has been discussed in the proposed numerical examples, as well as an assessment between the curve predicted by the model and that obtained from an experimental test has been presented. This last result seems very promising for the consistency of the model.

The model reproduces the structural behaviour of high-performance and/or fiber reinforced concrete members in bending. In particular, as the parameters are of easy physical meaning and of simple experimental evaluation, this model represents a very useful tool for the study of mechanical properties (strength and ductility) and of crack propagation regimes, according to concrete composition, typology and density of the fibers, distribution and characteristics of the longitudinal bars.

A very important result of the theoretical formulation is provided by the dependence of the structural behaviour on the member size. Only with the same brittleness numbers it is possible to obtain physically similar structural responses.

ACKNOWLEDGEMENTS

The present research was carried out with the financial support of the Ministry of University and Scientific Research (MURST), the National Research Council (CNR) and the EC-TMR Contract N° ERBFMRXCT960062.

References

1. Barenblatt, G.I. (1962). In: *Advances in Applied Mechanics*, pp.55-129, Dryden, H.L., von Karman, T. (Eds.), Academic Press, New York.
2. Willis, J.R. (1967) *J. Mech. Phys. Sol.* 15, 151.
3. Rice, J.R. (1968) *J. Appl. Mech.* 35, 379.
4. Mashall,D.B. Cox, B.N. and Evans, G.A. (1985) *Acta Metall. Mater.* 33, 2013.
5. Rose, L.R.F (1987) *Theor. Appl. Fract. Mech.* 7, 125.
6. Jenq, Y.S. and Shah, S.P. (1985) *J. Engng. Mech.* 111, 1227.
7. Carpinteri, A. (1984) *J. Struct. Engng.* 110, 544.
8. Bosco, C. and Carpinteri, A. (1992) *J. Engng. Mech.* 118, 1564.
9. Carpinteri, A. and Massabò, R. (1996) *Int. J. Fract.* 81, 125.
10. Carpinteri, A., Ferro, G. and Ventura, G. (2000). In: *Composite Materials & Structures*, pp.301-310, de Wilde, W.P., Blain, W.R., Brebbia, C.A. (Eds.). WIT Press, Southampton.
11. Okamura, H., Watanabe, K. and Takano, T. (1975) *Eng. Fract. Mech.* 7, 531.
12. Carpinteri, A. (1981) *Mat. and Struct.* 14, 151.
13. Carpinteri, A. and Massabò, R. (1997) *Int. J. Solids and Struct.* 34, 2321.
14. Ashour, S.A. and Wafa, F.F. (1993) *ACI Struct. J.* 90, 279.
15. Carpinteri, A. and Massabò, R. (1997) *J. Engng. Mech.* 123, 107.